The distinct behaviors of Pacific and Indian Ocean warm pool properties on seasonal and interannual time scales

Seon Tae Kim,[1] Jin-Yi Yu,[1] and Mong-Ming Lu[2]

[1] The seasonal and interannual variabilities of warm pool properties in the Pacific and Indian Ocean sectors are examined and contrasted. The properties examined are the size, mean and maximum sea surface temperatures (SSTs), and central position. The seasonal variability is more vigorous in the Indian Ocean sector, but the interannual variability is comparable in the Pacific and Indian Ocean sectors. The variability is associated with significant longitudinal and latitudinal displacements on seasonal time scales but only with longitudinal displacements on interannual time scales. As for the controlling factors, while the seasonal variability of the warm pool is controlled by the annual march of the Sun in the Pacific sector and by the Indian summer monsoon in the Indian Ocean sector, the interannual variability in both sectors is related mostly to El Niño–Southern Oscillation (ENSO). ENSO is closely correlated with the size variations and longitudinal displacements of the warm pool. Interestingly, the warm pool intensity in both sectors is not highly correlated with ENSO until 5 to 6 months after ENSO peaks. The possible causes of this delayed ENSO influence are discussed. Only size and intensity (i.e., mean SST) variations in the Indian Ocean warm pool are significantly correlated with quasi-biennial variability in the Indian monsoon, which indicates that the Indian Ocean warm pool may be a potential predictor for Indian monsoon variations.

1. Introduction

[2] The Indo-Pacific warm pool is an important feature of the climate system and is typically defined as the region of ocean enclosed by the 27.5°C or 28°C isotherm of sea surface temperature (SST) [e.g., *Wyrtki*, 1989; *Ho et al.*, 1995; *Fasullo and Webster*, 1999] which are threshold temperatures required for atmospheric deep convection [e.g., *Graham and Barnett*, 1987; *Zhang*, 1993; *Fu et al.*, 1994]. Through the excitement of deep convection, the warm pool is capable of influencing global climate via, for example, the Walker and Hadley circulations and serves as a major source of heat and water vapor [*Sardeshmukh and Hoskins*, 1988; *Webster and Lukas*, 1992]. Variations in the properties of the warm pool have been considered as a driving force to, as well as an indication of, climate variability and changes. For example, the warm pool size was suggested to be a key factor regulating tropical mean SSTs by *Pierrehumbert* [1995]. The extension of the warm pool is positively correlated with the occurrence of westerly wind bursts in the western Pacific, which are known to be important for the

onset of the El Niño events [*Eisenman et al.*, 2005]. Warm pool displacements and intensity variations are also known to affect the onset, intensity, and period of El Niño–Southern Oscillation (ENSO) [*Picaut et al.*, 1996; *Kessler*, 2001; *Sun*, 2003; *McPhaden*, 2004]. Changes in the warm pool size have been suggested to change the center of atmospheric deep convection, leading to local and remote changes in climate. *Williams and Funk* [2011] showed that a large warming trend in the Indian Ocean over the past 60 years has expanded the Indian Ocean warm pool westward and argued that this expansion has been instrumental in a shift of the sinking branch of the Walker circulation westward to eastern Africa, causing rainfall deficit there. It has also been suggested that warm pool SSTs may affect tropical cyclone frequency and intensity. *Webster et al.* [2005] showed that an increasing trend in the tropical cyclone number and intensity over the past 35 years could be associated with a warming trend in the north Indian Ocean and western Pacific Ocean. Slow fluctuations in warm pool SSTs were suggested to be capable of regulating decadal variability in the Hadley and Walker circulations [*Wang and Metha*, 2008]. Furthermore, the warming of the Indo-Pacific warm pool in recent decades was suggested as a contributor to a trend of intensification in the Hadley circulation [*Ma and Li*, 2008].

[3] Previous studies have improved our understanding of the Indo-Pacific warm pool, such as its surface energy balance and the relative roles played by atmospheric and oceanic processes in the balance [e.g., *Ramanathan and*

---

[1]Department of Earth System Science, University of California, Irvine, California, USA.
[2]Research and Development Center, Central Weather Bureau, Taipei, Taiwan.

Collins, 1991; *Wallace*, 1992; *Hartmann and Michelsen*, 1993; *Schneider et al.*, 1996; *Fasullo and Webster*, 1999; *Clement et al.*, 2005]. Most of the studies focused on the Pacific sector of the warm pool. Some of the studies that looked into the Indian Ocean sector of the warm pool indicated that the surface energy balance in this sector differs from that in the Pacific sector. *Schneider et al.* [1996] concluded from an examination of coupled atmosphere-ocean model simulations that on seasonal time scales, the solar penetration process affects the vertical temperature structure more in the Pacific than in the Indian Ocean. *Fasullo and Webster* [1999] found that the warm pool SST in the Indian Ocean is less sensitive to surface thermal forcing than it is in the Pacific. The warm pool in the Indian Ocean sector also has a stronger annual cycle than in the Pacific sector [*Fasullo and Webster*, 1999]. The warming trend in the warm pool since the 1970s has been about 2–3 times larger in the Indian Ocean sector than in the Pacific sector [*Williams and Funk*, 2011]. Coincident with the warming in the Indian Ocean, the mean strength of the Indian monsoon has weakened but its interannual variability has increased [*Goswami*, 2005]. It was also noted that the typical negative correlation between ENSO and the Indian monsoon has weakened in recent decades [*Kumar et al.*, 1999; *Kinter et al.*, 2002]. It has also been shown that the Indian Ocean warm pool is shallower than the Pacific warm pool [e.g., *Meng and Wu*, 2002]. Moreover, the Indian Ocean exhibits a unique interannual variability, which is called the Indian Ocean Dipole (IOD) [*Saji et al.*, 1999; *Webster et al.*, 1999], that may interfere with the Indian Ocean sector of the warm pool. These studies indicated that the warm pool properties and their variability in the Pacific and Indian Ocean sectors can be different and may play different roles in the climate system.

[4] In this study, we separate the Indo-Pacific warm pool into a Pacific sector and an Indian Ocean sector to examine and contrast their seasonal and interannual variability. We focus on variations in the warm pool intensity, size, and location. The warm pool intensity is often represented by the mean SST within the region where SSTs are greater than or equal to a threshold (which is usually set to be 28°C). Additionally, we also examine variations in the maximum SST inside the warm pool to see whether it is a good indicator of warm pool intensity. As for the warm pool location, previous studies have focused on the longitudinal displacement or the eastern boundary movement of the Pacific warm pool due to its close relation with the evolution of ENSO [e.g., *Picaut et al.*, 1996]. In this study, we examine the movement of the center of the warm pool by examining both its longitudinal and latitudinal displacements. This so-called "centroid" movement of the warm pool has been examined by *Ho et al.* [1995] using a short period (1982–1992) of satellite data, but that study focused only on the Pacific sector of the warm pool. For the size variations of the warm pool, we focus on its horizontal surface area, since a previous study by *Meng and Wu* [2002] showed that volume variations in both the Pacific and Indian Ocean sectors of the warm pool are similar to their surface area variations. Therefore, five particular properties of the warm pool are examined in this study: the horizontal size of the warm pool,

the mean and maximum SSTs inside the warm pool, and the central longitudinal and latitudinal locations of the warm pool.

2. Data Set and Method

[5] The SST data set used in this study is the National Oceanic and Atmospheric Administration (NOAA) Extended Reconstruction of Historical Sea Surface Temperature version 3 (ERSST v3) [*Smith et al.*, 2008] from the National Climate Data Center (NCDC). The data are available from 1854 to 2011 on $2° \times 2°$ grids and are produced by applying statistical methods to in situ and satellite observations. To test the sensitivity of the results to the SST data set used, we also examine the Met Office Hadley Centre Sea Ice and Sea Surface Temperature data set (HadISST) [*Rayner et al.*, 2003], which is reconstructed using an empirical orthogonal function and reduced space optimal interpolation [*Kaplan et al.*, 1998] and is available on $1° \times 1°$ grids from 1871 to 2011. We found the results to be similar and present only those produced from the ERSST data set here.

[6] Using SST data for the period 1950–2010, the size, maximum and mean SSTs, and the longitudinal and latitudinal locations of the center of the warm pool are calculated in the region enclosed by the 28°C isotherm within the region between 30°S–30°N and 30°E–130°W. We repeated our analyses with the warm pool defined by the 27.5°C isotherm, which has been used in some studies [e.g., *Graham and Barnett*, 1987] to define warm pool, but found little difference. Only the results with the warm pool defined by the 28°C isotherm are shown. In this study, the warm pool is separated into Pacific and Indian Ocean sectors (see Figure 2) based on the basin mask information from NOAA's National Oceanographic Data Center [*Locarnini et al.*, 2010]. The boundary (i.e., the red dashed line in Figure 2) of the two sectors connects the Indonesian island chain from the southern tip of the Indo-China Peninsula to the northern tip of the Australia. For the sake of discussion, these two sectors are referred to as the Indian Ocean warm pool and the Pacific warm pool, respectively. The central latitudinal and longitudinal locations of the warm pool are calculated using the following methods:

$$\mathrm{X}_{center} = \sum_{i=1}^{n} x_i/n \ \text{ and } \ \mathrm{Y}_{center} = \sum_{i=1}^{n} y_i/n,$$

where x and y are the longitudinal and latitudinal locations, respectively, of SST data grids inside the region enclosed by the 28°C isotherm, and n is the total number of grid points inside the warm pool. Latitudinal weighting (i.e., the squared root of cos(latitude)) is considered in the calculation of the central locations.

[7] To examine the relationship between the warm pool properties and the Indian monsoon for the period 1950–2010, we use the All-India Rainfall (AIR) [*Parthasarathy et al.*, 1994] index for the period 1950–2010 to examine the monsoon–warm pool relationships. The AIR, which is available from 1871 onward, was compiled by the Indian
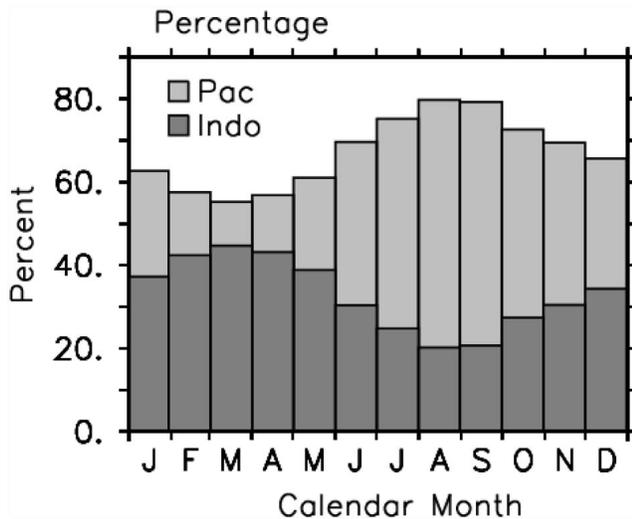
Figure 1. The seasonal evolution of the percentages of the Indo-Pacific warm pool in the Pacific and Indian Ocean sectors.

Institute of Tropical Meteorology using an area-weighted surface rainfall data set from 306 stations within India.

3. Seasonal Variations of the Warm Pool Properties

[8] We first examine how the Indo-Pacific warm pool moves between the Pacific and Indian Ocean sectors during its seasonal evolution. Figure 1 shows the respective percentages of the surface area of the warm pool within each of the sectors. It shows that the Pacific sector is always the dominant part of the warm pool throughout the year, but the warm pool moves more into the Pacific Ocean during boreal summer and more into the Indian Ocean during boreal spring. In August, the Pacific sector comprises 80% of the Indo-Pacific warm pool while the Indian Ocean sector comprises only 20%. In March, as much as 45% of the warm pool is located within the Indian Ocean. The variations in the area percentage are further examined using the monthly climatology of the warm pool SSTs in Figure 2. In both sectors, the warm pool moves northward during boreal summer and southward during boreal winter, following the annual march of the Sun. The Pacific warm pool reaches its largest size when it is at its northernmost latitude near the end of the boreal summer (September; Figure 2i) and its smallest size when it is at its southernmost latitude near the end of boreal winter (February; Figure 2b). Although similar latitudinal excursions occur in the Indian Ocean, the size variations in this sector are larger than those in the Pacific sector and differ in their evolution. Instead of having a maximum size in boreal summer as in the Pacific sector, the warm pool in the Indian Ocean sector is smallest in August–September. This is related to the fact that the Indian Ocean is uniquely bounded to the north by the Asian continents, which adds the Indian monsoon as an additional factor controlling the Indian Ocean warm pool size. The southwesterly monsoon during boreal summer induces coastal upwelling and enhances surface evaporation cooling in the western Arabian Sea, thereby shrinking the warm pool to a

small area in the northeastern corner of the Indian Ocean (Figures 2g–2i). This is the time that the Indian Ocean sector constitutes the smallest percentage of the Indo-Pacific warm pool in Figure 1. It is during the two intermonsoon seasons (i.e., boreal spring and autumn) that the Indian Ocean warm pool has relatively large size. Particularly in boreal spring, the warm pool covers most of the northern Indian Ocean, and the percentage of the warm pool in the Indian Ocean sector reaches its maximum value (Figure 1). The seasonal variations shown in Figures 1 and 2 suggest that the seasonal displacement of the warm pool between the Pacific and Indian Oceans is controlled by two factors: the annual march of the solar heating and the Indian summer monsoon.

[9] In Figures 3a–3e, we examine the seasonal variations of five warm pool properties: horizontal size, longitudinal and latitudinal positions, mean SST, and maximum SST. Values shown are the deviations from the respective annual means. Harmonic analyses are applied to the variations (shown in Figures 3f–3j) to determine whether the variations are dominated by the annual or semiannual harmonics. Figures 3a and 3f indicate that the size variations of the warm pool (as a percentage of the annual mean) in both the Pacific and Indian Ocean sectors are dominated by the annual harmonics, consistent with the discussion in connection with Figure 2, but owing to differences in the phase of these two annual harmonics, the size variation of the entire Indo-Pacific warm pool is dominated by semiannual harmonics. The Indo-Pacific warm pool expands to its maximum size in April when the Indian Ocean sector of the warm pool reaches its largest size and its secondary maximum in October when the Pacific sector reaches its maximum size. The Indo-Pacific warm pool contracts to its smallest size in January when the Pacific warm pool is at its smallest. The secondary minimum of the Indo-Pacific warm pool occurs in August when the Indian Ocean warm pool is at its smallest due to the summer monsoon-induced cooling, which is partially compensated for by the expanding Pacific warm pool. It is obvious from Figure 3a that the seasonal size variations of the Indo-Pacific warm pool follow more closely with the size variations in the Indian Ocean sector than with the variations in the Pacific sector.

[10] The seasonal displacements in longitude and latitude of the center of the warm pool are shown in Figures 3b and 3c, where positive (negative) deviations represent eastward (westward) or northward (southward) displacements from the annual mean locations. The most obvious feature in Figure 3c is that the warm pool migrates northward from boreal winter to summer and southward from boreal summer to winter in both the Pacific and Indian Ocean sectors. The displacements are overwhelmingly dominated by the annual harmonics (Figure 3h) and are almost identical in amplitude in the two sectors (about $\pm 7°$), although the northward displacement in the Indian Ocean during summer is limited by the Asian continent. Figures 3b and 3g show that the longitudinal displacement of the warm pool is also dominated by the annual harmonics in both the Pacific and Indian Ocean sectors; however the displacements are in opposite directions. The warm pool in the Indian Ocean displaces westward as it expands in boreal spring and displaces eastward as it shrinks in boreal summer. As for the Pacific sector, the warm pool displaces eastward during boreal winter and spring, which is related to the eastward expansion of the
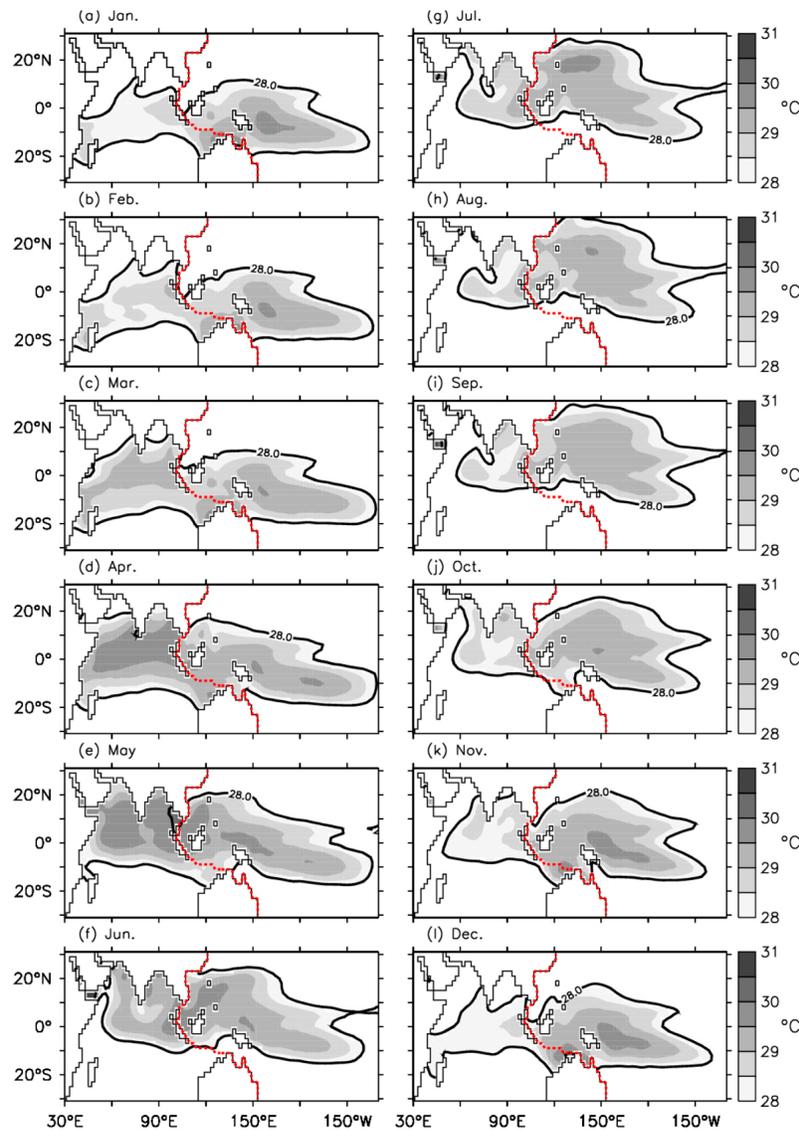
Figure 2. The monthly climatology of the Indo-Pacific warm pool SSTs. Values shown are the monthly mean SSTs greater than 28°C; the threshold used to define the Indo-Pacific warm pool. The boundary between the Pacific and Indian Ocean sectors of the warm pool is indicated by a red dashed line.

southern branch of the Pacific warm pool during the austral summer as shown in Figure 2. The southern branch retreats westward toward the Dateline by the end of austral winter (i.e., August). Figure 3b indicates that the longitudinal displacement of the warm pool is dominated by the boreal seasonal cycle (i.e., the Indian monsoon) in the Indian Ocean sector but by the austral seasonal cycle in the Pacific sector. In both sectors, the center of the warm pool displaces about $\pm 8°$ in longitude during the course of the year. The longitudinal variations of the Indo-Pacific warm pool follow more closely those of the Indian Ocean sector, due to the larger size variations in this sector.

[11] Next we examine the seasonal variations in the warm pool intensity. We focus on two quantities: the mean SST (Figure 3d) and the maximum SST (Figure 3e) within the warm pool. The annual mean values of the mean SST in the Pacific (28.9°C) and Indian Ocean (28.7°C) sectors of the warm pool are almost the same. The mean SST in the Pacific sector varies little throughout the year (Figure 3d) and is dominated by a weak semiannual harmonic (Figure 3i). The peak values occur in boreal spring and autumn when the Sun is directly overhead at the equator. In contrast, the mean warm pool SST in the Indian Ocean sector experiences a relatively large seasonal variation with a maximum excursion of more than 0.5°C. The variation is dominated by an annual harmonic with the largest deviation in April, which is the time when the Indian Ocean warm pool expands to its maximum size (see Figure 3a). The mean SST in this sector decreases from July to December, which also coincides with the period of time when the Indian Ocean warm pool shrinks. Seasonal variations in the warm pool size and intensity (i.e., mean SST) are positively correlated in the Indian Ocean sector, with a correlation coefficient of 0.67 that is significant at a 95% level according to a Student's t test. No such a significant positive correlation is found in the Pacific warm pool (the correlation coefficient is 0.43). The
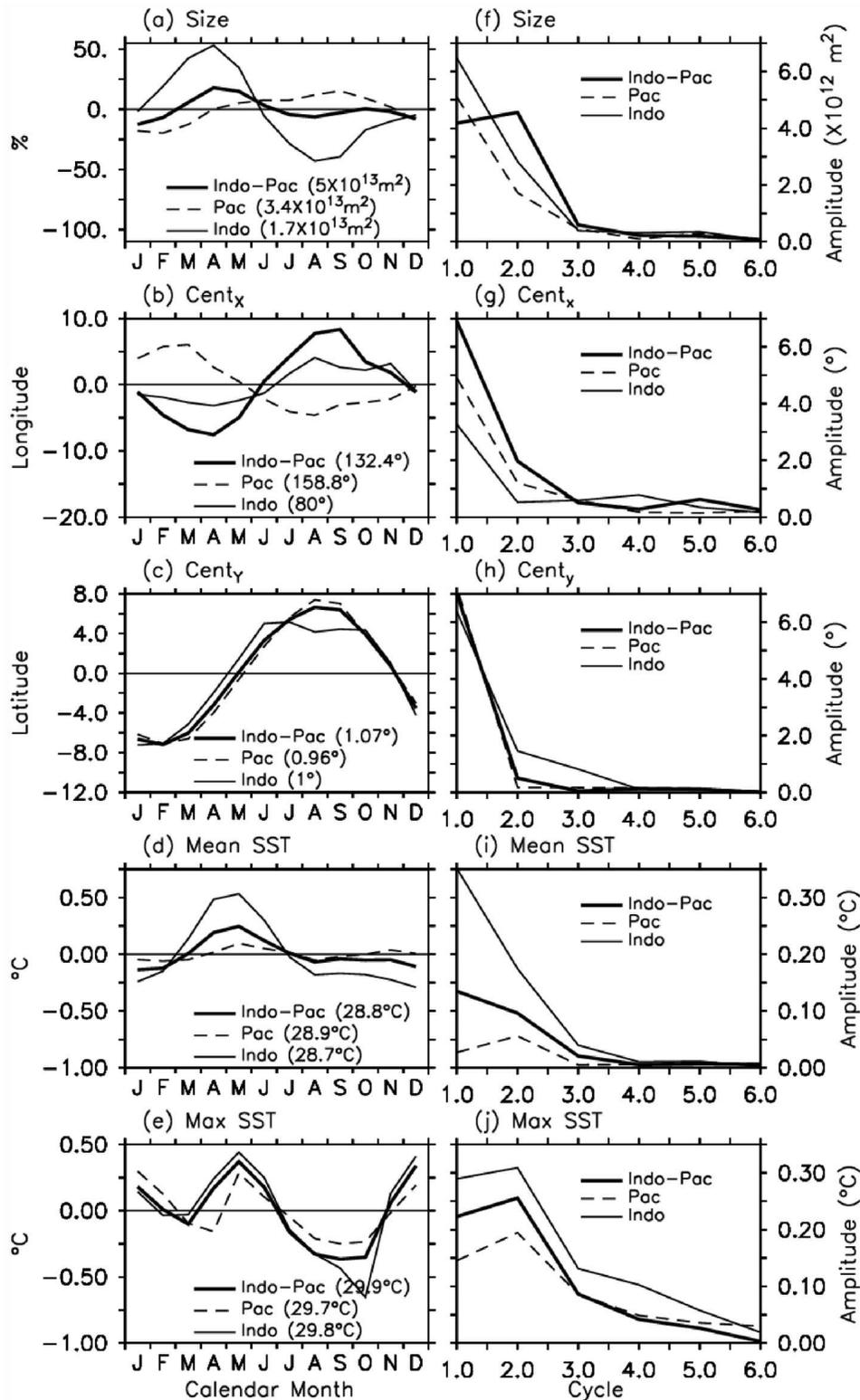
Figure 3. (left) The seasonal cycle and (right) its harmonics of warm pool properties: (a, f) horizontal size, (b, g) the longitudinal displacement, (c, h) the latitudinal displacement, (d, i) mean SST, and (e, j) maximum SST. Thick solid lines represent values for the Indo-Pacific warm pool, thin dashed lines represent values for the Pacific warm pool, and thin solid lines represent values for the Indian Ocean warm pool.
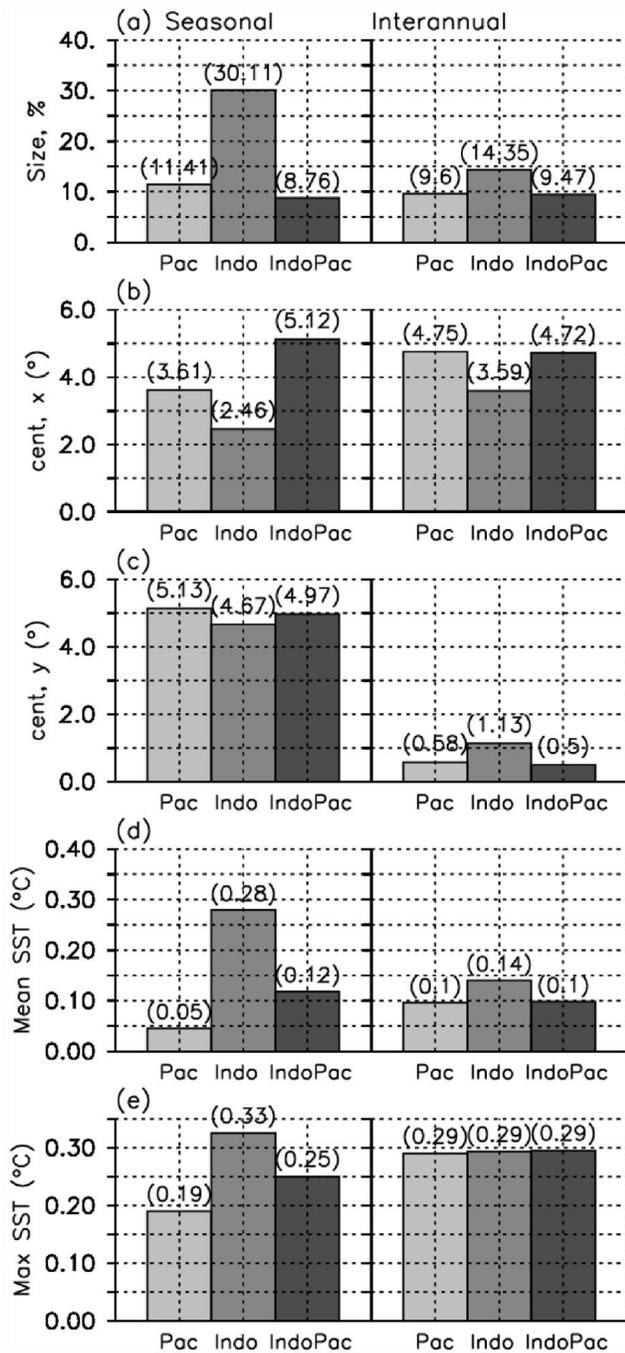
Figure 4. Standard deviations of (left) seasonal and (right) interannual variability of (a) horizontal size, (b) the longitudinal displacement, (b) the latitudinal displacement, (d) mean SST, and (e) maximum SST for the Pacific and Indian Ocean sectors and the total warm pool. Values of the standard deviations are shown in parentheses on top of the bars.

seasonal variations of the mean SST in the Indo-Pacific warm pool follow those of the Indian Ocean warm pool. As indicated in Figure 3j, the maximum values of the warm pool SST in both the Pacific and Indian Ocean sectors are dominated by the semiannual harmonics, with the peak values occurring near the boreal late spring and early winter, which reflects the influence from the annual march of the

solar heating and indicates that the maximum SST values of the warm pool are not well linked to the other four warm pool properties on seasonal time scales.

[12] The analyses presented in Figure 3 together indicate that the seasonal variability of warm pool size and intensity is more vigorous in the Indian Ocean sector than in the Pacific sector, while the longitudinal and latitudinal displacements of the warm pool are comparable in the two sectors. The standard deviations of the seasonal cycle shown in Figures 4a–4e lend further support to this conclusion. The standard deviation of the size variation is about 30% for the Indian Ocean sector but only 11% for the Pacific sector, which is a statistically significant difference at the 95% level based on F test. The differences between the two sectors in the seasonal variability of the mean SST and the maximum SST of the warm pool are also statistically significant. The seasonal variations in the warm pool size, intensity, and longitudinal displacement in the Indian Ocean sector are closely linked to each other by the monsoon: the stronger the warm pool intensity, the larger the warm pool size, and the greater the westward expansion of the warm pool. In contrast, the intensity of the Pacific warm pool varies little throughout the year, although the center of the Pacific warm pool undergoes seasonal variations comparable to those of the Indian Ocean warm pool. These contrasting features indicate the warm pool SST is more strongly regulated by dynamical and thermodynamical processes [e.g., *Clement et al.*, 2005; *Ramanathan and Collins*, 1991] in the Pacific sector than in the Indian Ocean sector.

4. Interannual Variations of the Warm Pool Properties

[13] We next examine the magnitudes of the interannual variability of the warm pool in the Pacific and Indian Ocean sectors. Interannual anomalies are obtained by applying a 3 month running mean to the warm pool properties after their monthly climatology and trends are removed. We first compare the standard deviations of the interannual variations to those of the seasonal variations in Figure 4. Figure 4a shows that the interannual variability in the Pacific warm pool size is comparable to the seasonal variability, but the interannual variability in the Indian Ocean sector is less than half of its seasonal variability. The interannual variability in the warm pool size is now comparable in the two sectors. Figures 4b and 4c show that the interannual variability of the warm pool is associated with large longitudinal displacements but small latitudinal displacements in both sectors. The longitudinal displacement is particularly large in the Pacific sector. Figure 4d shows that the interannual variations of the Pacific warm pool are accompanied by significant variations in the mean SST, which is also different from its seasonal variations. The interannual variability in the mean SST of warm pool is comparable in the Pacific and Indian Ocean sectors. Figure 4e shows that the interannual variability of the maximum SST is also comparable in these two sectors. The comparisons presented in Figure 4 indicate that although the Indian Ocean sector dominates the seasonal variability of the Indo-Pacific warm pool, the interannual variability in the Pacific and Indian Ocean sectors are comparable. Furthermore, while the warm pool variability is associated with both longitudinal and latitudinal

Table 1. Correlation Coefficients of Warm Pool Properties in the Pacific and Indian Ocean Sectors of the Warm Pool and the Niño3.4 Index[a]

Warm Pool Properties	Pacific Ocean			Indian Ocean		
	Monthly	JAS	DJF	Monthly	JAS	DJF
Size	**0.79**	**0.75**	**0.87**	**0.45**	0.21	**0.64**
Centroid, x	**0.88**	**0.89**	**0.94**	−0.35	−0.33	−0.39
Centroid, y	−0.15	−0.60	0.04	0.22	0.10	**0.39**
Mean SST	0.21	−0.18	**0.44**	**0.38**	0.18	**0.58**
Maximum SST	0.08	−0.16	0.00	0.12	−0.09	0.14

[a]The correlation coefficients are obtained using whole monthly values and July–August–September (JAS) and December–January–February (DJF) seasonally averaged values. Coefficients that are significant at 95% according to Student's t test are bold.

displacements on seasonal time scales, the variability is associated predominantly with longitudinal displacements on interannual time scales. It is important to note that for the entire Indo-Pacific warm pool, the interannual variability is comparable to the seasonal variability in size, longitudinal displacement, mean SST, and maximum SST. Only for the latitudinal displacement, is the interannual variability significantly smaller than the seasonal variability.

[14] There are at least two possible contributors to interannual variability in the Indo-Pacific warm pool: ENSO and monsoon. We now look into their respective contributions to warm pool variability in each of the two ocean sectors. To investigate the relationship between the warm pool and ENSO, in Table 1 we display the correlation coefficients between monthly warm pool properties and the monthly Niño3.4 SST index (SST anomalies averaged in the region between 5°N–5°S and 170°W–120°W). Table 1 shows that ENSO is significantly correlated (at the 95% level) with the size variations and longitudinal displacements of the Pacific warm pool. El Niño events increase the size of the Pacific warm pool and shift the center of the warm pool eastward, vice versa for La Niña events. ENSO accounts for about 63% of the interannual variability in warm pool size and about 78% of that in longitudinal displacement. We also calculate the correlation coefficients for boreal summer (July–August–September; JAS) and winter (December–January–February; DJF). As shown in Table 1, the correlations between Niño3.4 and warm pool size and longitudinal displacement are significant in both seasons. Since ENSO typically develops in summer and peaks in winter, Table 1 indicates that the significant correlations of ENSO with the warm pool size and longitudinal displacement persist throughout its lifecycle.

[15] Table 1 also indicates that ENSO is not significantly correlated with interannual variations in the Pacific warm pool intensity (i.e., the mean and maximum SSTs). The weak correlation with the Pacific warm pool intensity can be understood by looking at the typical SST anomaly pattern in the Indo-Pacific Ocean during ENSO events, as shown in Figure 5. This pattern is obtained by regressing Indo-Pacific SST anomalies with the Niño3.4 SST index for JAS and DJF. It is evident from Figure 5 that while SSTs in the eastern half of the Pacific warm pool (the outline of the warm pool is indicated in Figures 5e–5h by black counter) increase, there are negative SST anomalies in the western half of the Pacific warm pool. As a result of this partial

cancellation, the warming effect of El Niño (or the cooling effect of La Niña) is not well reflected in the mean SST and maximum SST. It is noticed that the magnitude of the SST anomalies in the far western Pacific does not change much when the SST anomalies increase in the eastern to central Pacific during the development of the El Niño or La Niña event from JAS to DJF. Therefore, the cancellation effect is weaker in DJF when ENSO events peak. This is consistent with Table 1 that shows the mean SST in the warm pool has a significant correlation with ENSO in DJF.

[16] Table 1 also shows that although ENSO's correlation with the latitudinal displacement of the Pacific warm pool is not statistically significant for the entire calendar year, the correlation is significant in boreal summer. To further understand this correlation, we show in Figures 5e–5h the outline of the seasonal warm pool and the outline of the warm pool corresponding to four standard deviations (STDs) of Niño3.4 index. The four STDs are used in Figure 5 to amplify the ENSO influences on the warm pool displacement. Figure 5 shows that while the Pacific warm pool expands and contracts during ENSO mainly via longitudinal displacements, the latitudinal profile of the warm pool surface does change. The change is particularly obvious in JAS during the time when the Pacific warm pool is located near the equator and both the northern and southern branches of the warm pool (i.e., the warm waters that coincide with the Inter-Tropical Convergence Zone and the South Pacific Convergence Zone, respectively) are influenced by ENSO. Between these two branches, the southern branch contains a larger surface area of warm water than the northern branch. The southern branch extends eastward during El Niño and retreats westward during La Niña. As a result, the percentage of the surface area of the warm pool in the southern branch increases during El Niño and decreases during La Niña. Therefore, the latitudinal center of the Pacific warm pool shifts southward during El Niño and northward during La Niña. This explains why Table 1 shows a significant negative correlation between the latitudinal displacement of the Pacific warm pool and ENSO in JAS. During DJF, the southern branch of the Pacific warm pool moves southward extending to 20°S and is less influenced by ENSO warming and cooling, and thus the weak correlation with the Niño3.4 index (see Table 1).

[17] As for the Indian Ocean sector of the warm pool, Table 1 shows that ENSO has a remote influence on the size, intensity, and longitudinal displacement of the Indian Ocean warm pool with the correlation coefficients significant at 95% level. Particularly, the significant correlation with the intensity of the Indian Ocean warm pool is a distinctive feature that is not found for the Pacific warm pool. When the correlation is separately estimated for JAS and DJF, ENSO's correlations with the size and intensity of the Indian Ocean warm pool are significant in DJF (i.e., the peak phase of ENSO). We find from Figures 5c and 5d that the stronger winter correlations are related to a basin-wide warming and cooling of the Indian Ocean during the mature phase of ENSO events. It is known that the Indian Ocean tends to warm up (cool down) basin wide after an El Niño (La Niña) event peaks due to the ENSO-induced heat flux anomalies [*Klein et al.*, 1999] and ocean Rossby wave propagation [*Xie et al.*, 2002]. This basin-wide warming/cooling typically peaks in late boreal winter and early spring and this explains
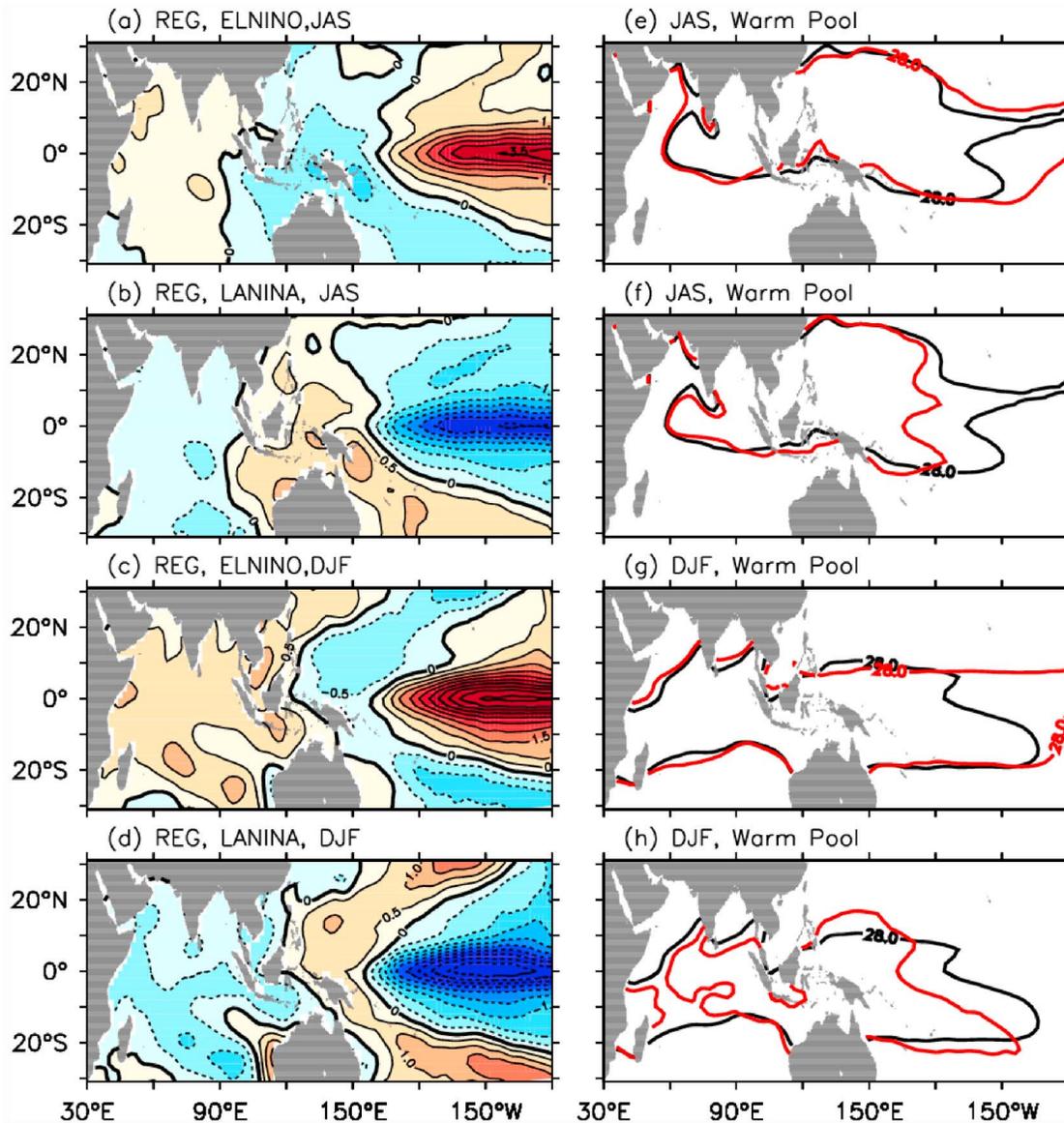
Figure 5. Spatial patterns of (left) SST anomalies (SSTA) and (right) the warm pool. They are obtained separately for (a, c, e, g) El Niño and (b, d, f, h) La Niña phases and for JAS (Figures 5a, 5b, 5e, and 5f) and DJF (Figures 5c, 5d, 5g, and 5h) averaged values. The SSTA spatial patterns are produced by multiplying a four standard deviation (SD) of the Niño3.4 index to the regression of the SSTA on the Niño3.4 SST index. The black 28°C isotherm of SST represents the JAS and DJF climatology, and the red isotherm represents the sum of the climatology and regressed SSTA multiplied by four SD.

why ENSO's correlation with the warm pool intensity is large and significant in DJF. The basin-wide warming (cooling) during El Niño (La Niña) expands (shrinks) the Indian Ocean warm pool and also explains why the size of the Indian Ocean warm pool is significantly correlated with the ENSO during DJF (see Table 1). The correlation analysis also indicates that the longitudinal displacement of the Indian Ocean warm pool due to ENSO is in an opposite direction from that of the Pacific warm pool with significant correlation persisting from the ENSO development to its peak. The opposite longitudinal displacement between the two sectors during ENSO can be attributed to the opposite directions of the Pacific and Indian Ocean branches of the global Walker circulation.

[18] To further explore the cause-and-effect relations between ENSO and warm pool variations, their lead-lag correlations are calculated and shown in Figure 6. For the Pacific warm pool (Figure 6a), the largest correlations occur when ENSO (i.e., the Niño3.4 SST index) leads the warm pool size by 1 month. It is also noticed that about 5 months after ENSO reaches its mature stage the Pacific warm pool mean SST reaches its peak value. This may be the time when the SST anomalies in the western Pacific that are out of phase with the ENSO SST anomalies diminish. The longitudinal displacement of the Pacific warm pool occurs almost simultaneously with the development of the ENSO. As for the Indian Ocean sector (Figure 6b), the warm pool is displaced to the west simultaneously during the ENSO
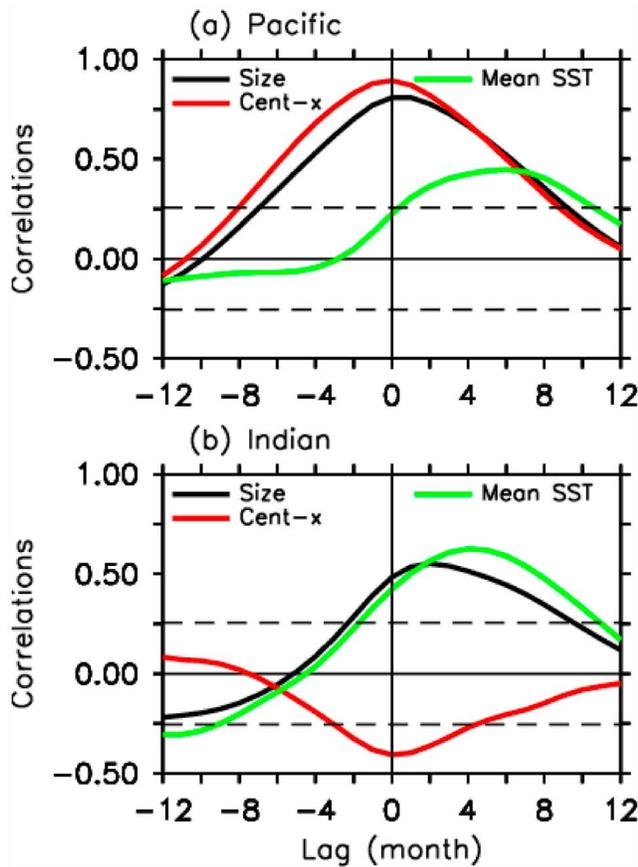
Figure 6. Lead-lag correlations between the Niño3.4 indices and warm pool properties for (a) the Pacific sector and (b) the Indian Ocean sector on interannual time scales. The warm pool properties analyzed are the size (black), longitudinal displacement (red), and mean SST (green). Positive lags indicate that the ENSO leads the warm pool properties. Correlations significant at the 95% confidence level are indicated by the horizontal dashed lines.

development while the warm pool size reaches its peak 2 months after ENSO peaks. Figure 6b also shows that the mean SST of the Indian Ocean warm pool is affected remotely by ENSO with a lag time of 4 months. As mentioned, the enhanced warm pool mean SST during El Niño is related to the Indian Ocean basin-wide warming, which is known to reach its maximum about one season after El Niño peaks [*An*, 2004; *Yu and Lau*, 2005]. The El Niño-induced tropical Indian Ocean warming can persist through the spring and early summer after ENSO dissipates and can prolong ENSO's influence on the climate of the Indian and western Pacific region [e.g., *Annamalai et al.*, 2005; *Yang et al.*, 2007; *Xie et al.*, 2009, 2010; *Du et al.*, 2009, 2011]. This so-called capacitor effect of the Indian Ocean may also explain the lagged response to ENSO of the mean SST in the Pacific and Indian Ocean sectors of the warm pool.

[19] We also examine the relationship between the Indian monsoon and warm pool properties. Figures 7a–7e display the lead-lag correlations between the June–July–August (JJA) AIR index and the warm pool properties. Figure 7 shows that the Indian monsoon rainfall is more highly correlated with the warm pool variability in the Indian Ocean
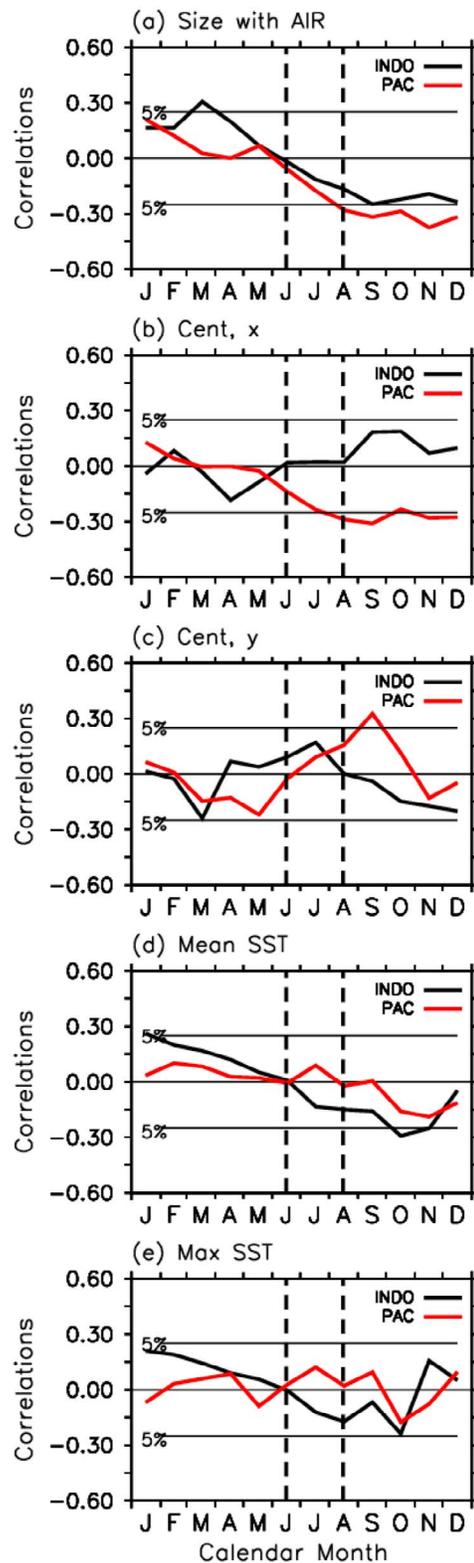

Figure 7. Correlations of the June–July–August All-India Rainfall (AIR) index with the warm pool properties: (a) size, (b) longitudinal displacement, (c) latitudinal displacement, (d) mean SST, and (e) maximum SST of the Pacific (red) and Indian Ocean (black) warm pool. Correlations significant at the 95% confidence level are indicated by the horizontal dashed lines.
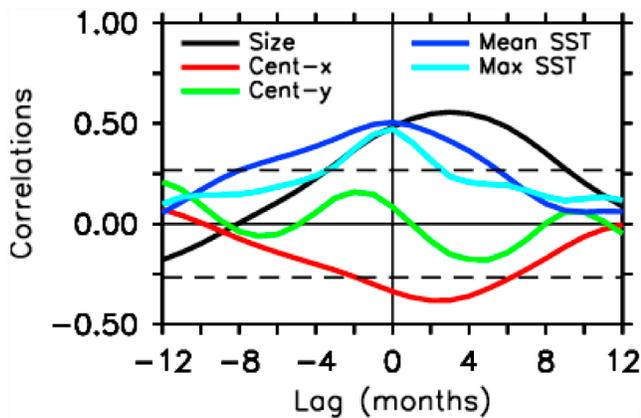
Figure 8. Lead-lag correlations of warm pool properties in the Pacific and Indian Ocean sectors. Correlations significant at the 95% confidence level are indicated by the horizontal dashed lines. Positive lags indicate that the Pacific warm pool leads the Indian Ocean warm pool.

sector (the black curves) than with that in the Pacific sector (the red curves). Correlations of the Indian monsoon with the Pacific warm pool are mostly not statistically significant at the 95% level. The size of the Indian Ocean warm pool has a positive correlation with the monsoon variability during the seasons preceding the summer monsoon and a negative correlation after the monsoon season (Figure 7a). A similar lead-lag correlation is also found with the mean SST of the Indian Ocean warm pool (Figure 7d). These relations indicate that a stronger than normal Indian summer monsoon is preceded by an expanding and warming Indian Ocean warm pool in boreal spring and followed by a shrinking and cooling Indian Ocean warm pool in boreal autumn. It is likely that the larger size and warmer Indian Ocean warm pool can supply more moisture into the Indian Peninsula to produce a stronger summer monsoon, thereby producing stronger surface winds over the Indian Ocean, enhancing surface evaporation and acting to cool down the warm pool afterward. These cyclic feedback processes between the monsoon and the Indian Ocean warm pool take about 2 years, according to the interval between the largest positive and negative correlations shown in Figure 7a and 7d. This result indicates that the correlation between the Indian Ocean warm pool and monsoon is strong on the biennial time scale, which is consistent with *Li et al.* [2001], who argued that the strength of the Indian monsoon is affected more by the Indian Ocean in the 2–3 year band but by ENSO on other interannual time scales. The cause of this strong biennial correlation may be the local monsoon-ocean interactions proposed as the source of the so-called Tropospheric Biennial Oscillation (TBO) [*Meehl*, 1987, 1993] or by remote influences from the biennial component of ENSO on both the monsoon and the Indian Ocean [*Fasullo*, 2004].

[20] Figures 7b and 7c show that size variations in the Indian Ocean warm pool are associated with both longitudinal and latitudinal displacements of the center of the warm pool although the correlations do not exceed the 95% significance level. Preceding a stronger than normal Indian summer monsoon, the Indian Ocean warm pool expands into the western (Figure 7b) and northern (Figure 7c) Indian

Ocean. Conversely, after the strong monsoon, the warm pool retracts into the eastern and southern Indian Ocean. Also, summer monsoon rainfall is only weakly correlated with the maximum SST (Figure 7e) in the Indian Ocean sector of the warm pool. Therefore, it is interesting to note that the Indian monsoon can affect the Indian Ocean warm pool intensity (i.e., mean SST) on both seasonal and interannual time scales. The biennial variability of the monsoon is closely correlated with the size and mean SST of the Indian Ocean warm pool.

[21] We also looked into the lead-lag correlations between the warm pool properties and the IOD. Following *Saji et al.* [1999], an IOD index is defined as the difference in SST anomaly between the tropical western Indian Ocean (50°E–70°E, 10°S–10°N) and the tropical southeastern Indian Ocean (90°E–110°E, 10°S–0°). We found that the largest correlation coefficients (which are significant at the 95% level) occur when the IOD leads the size and the longitudinal location of Indian Ocean warm pool by about 2–3 months. The correlations (not shown) indicate that the Indian Ocean warm pool expands toward the west after a positive phase of the IOD and contracts toward the east after a negative phase of the IOD. No significant correlations are found with other properties of the Indian Ocean warm pool or properties of the Pacific warm pool. Apparently, the influence of the IOD is limited to the Indian Ocean warm pool despite the global climate impacts of the IOD that have been reported in several studies [e.g., *Saji and Yamagata*, 2003; *Guan and Yamagata*, 2003].

[22] Last, in Figure 8 we examine the lead-lag correlations between the Pacific and Indian Ocean sectors of the warm pool. Figure 8 shows that these two sectors are significantly correlated for the variations in size, longitudinal displacement, and intensity (both the mean SST and the maximum SST). The largest correlation coefficients occur when the size and the longitudinal displacement of the Pacific warm pool lead those of the Indian Ocean warm pool by 3 months. These correlations are consistent with the timing of the Pacific and Indian Ocean warm pool responses to ENSO as discussed previously (see Figure 6). The warm pool intensity (e.g., mean and maximum SST) in both sectors varies almost simultaneously due to their similar delayed responses to ENSO warming/cooling as discussed in connection with Figure 6. Figure 8 shows that the interactions between the Pacific and Indian Ocean sectors of the warm pool are results of ENSO forcing.

5. Summary and Discussion

[23] This study examined the seasonal and interannual variations of five Indo-Pacific warm pool properties (size, mean and maximum SSTs, and latitudinal and longitudinal center) and contrasted the variability in the Pacific and Indian Ocean sectors. We conclude that variations in the warm pool are dominated by the Indian Ocean sector on seasonal time scales but that both sectors contribute significantly to the interannual variability. On seasonal time scales, the Pacific warm pool expands and contracts by only about 15% of its annual mean size at the most, while the Indian Ocean warm pool varies in size by as much as 50%. The large variations in the Indian Ocean sector are related to strong local influences from the Indian summer monsoon.

The size variations in both sectors are accompanied by large latitudinal displacements of the warm pool, which are controlled by the annual march of the Sun. The longitudinal displacements of the warm pool is not as large as the latitudinal displacements and are found to be controlled by the seasonal cycle of the monsoon in the Indian Ocean sector, and by the austral seasonal cycle in the Pacific sector.

[24] On interannual time scales, the magnitude of the warm pool variability in the entire Indo-Pacific warm pool is similar to the magnitude of the seasonal variability. In contrast to the seasonal variability, the interannual variability is associated with large longitudinal displacements but small latitudinal displacements. ENSO is the primary contributor to the interannual variability in both sectors. When an El Niño event develops, the size of the warm pool increases as it extends eastward in the Pacific sector and westward in the Indian Ocean sector, and vice versa for a La Niña event. This study finds that the response of the warm pool intensity to ENSO does not reach its peak until about 5 months after ENSO peaks. The delay in the Indian Ocean is due to the time required for ENSO-induced basin-wide warming/cooling to develop. The delay in the Pacific is due to an out-of-phase SST anomaly that develops in the western half of the Pacific warm pool that partially cancels out the warming (cooling) effects associated with El Niño (La Niña) events in the eastern half. This cancellation effect diminishes gradually about 5–6 months after ENSO peaks. Therefore, this study finds that the intensity of ENSO, which tends to peak in boreal winter, may be reflected in the Pacific or Indian Ocean warm pool intensity during the following boreal spring. Finally, the quasi-biennial variability of the Indian monsoon, which is known as the TBO, is also found to have strong interactions with the Indian Ocean warm pool. The positive phase of the TBO (i.e., stronger than normal summer monsoon) is preceded by an expanding and warming Indian Ocean warm pool and followed by a shrinking and cooling warm pool. The correlation implies that the interannual variations in both size and mean SST in the Indian Ocean warm pool have the potential to be utilized for the prediction of Indian monsoon variations.

References

An, S.-I. (2004), A dynamic link between the basin-scale and zonal modes in the tropical Indian Ocean, *Theor. Appl. Climatol.*, *78*, 203–215, doi:10.1007/s00704-003-0027-2.

Annamalai, H., S.-P. Xie, J.-P. McCreary, and R. Murtugudde (2005), Impact of Indian Ocean sea surface temperature on developing El Niño, *J. Clim.*, *18*, 302–319, doi:10.1175/JCLI-3268.1.

Clement, A. C., R. Seager, and R. Murtugudde (2005), Why are there tropical warm pools?, *J. Clim.*, *18*, 5294–5331, doi:10.1175/JCLI3582.1.

Du, Y., S.-P. Xie, G. Huang, and K. Hu (2009), Role of air-sea interaction in the long persistence of El Niño–induced north Indian Ocean warming, *J. Clim.*, *22*, 2023–2038, doi:10.1175/2008JCLI2590.1.

Du, Y., L. Yang, and S.-P. Xie (2011), Tropical Indian Ocean influence on northwest Pacific tropical cyclones in summer following strong El Niño, *J. Clim.*, *24*, 315–322, doi:10.1175/2010JCLI3890.1.

Eisenman, I., L. Yu, and E. Tziperman (2005), Westerly wind bursts: ENSO's tail rather than the dog?, *J. Clim.*, *18*, 5224–5238, doi:10.1175/JCLI3588.1.

Fasullo, J. (2004), Biennial characteristics of Indian monsoon rainfall, *J. Clim.*, *17*, 2972–2982, doi:10.1175/1520-0442(2004)017<2972: BCOIMR>2.0.CO;2.

Fasullo, J., and P. J. Webster (1999), Warm pool SST variability in relation to the surface energy balance, *J. Clim.*, *12*, 1292–1305, doi:10.1175/1520-0442(1999)012<1292:WPSVIR>2.0.CO;2.

Fu, R., A. D. Del Genio, and W. B. Rossow (1994), Influence of ocean surface conditions on atmospheric vertical thermodynamic structure and deep convection, *J. Clim.*, *7*, 1092–1108, doi:10.1175/1520-0442(1994)007<1092:IOOSCO>2.0.CO;2.

Goswami, B. N. (2005), The Asian monsoon: Interdecadal variability, in *The Global Monsoon System: Research and Forecast*, edited by C.-P. Chang, B. Wang, and N.-C. G. Lau, pp. 455–471, World Meteorol. Org., Geneva, Switzerland.

Graham, N. E., and T. P. Barnett (1987), Sea surface temperature, surface wind divergence, and convection over tropical oceans, *Science*, *238*, 657–659, doi:10.1126/science.238.4827.657.

Guan, Z., and T. Yamagata (2003), The unusual summer of 1994 in East Asia: IOD teleconnections, *Geophys. Res. Lett.*, *30*(10), 1544, doi:10.1029/2002GL016831.

Hartmann, D. L., and M. L. Michelsen (1993), Large-scale effects on the regulation of tropical sea surface temperature, *J. Clim.*, *6*, 2049–2062, doi:10.1175/1520-0442(1993)006<2049:LSEOTR>2.0.CO;2.

Ho, C.-R., X.-H. Yan, and Q. Zheng (1995), Satellite observations of upper-layer variabilities in the western Pacific warm pool, *Bull. Am. Meteorol. Soc.*, *76*, 669–679, doi:10.1175/1520-0477(1995)076<0669: SOOULV>2.0.CO;2.

Kaplan, A., M. A. Cane, Y. Kushnir, A. C. Clement, M. B. Blumenthal, and B. Rajagopalan (1998), Analyses of global sea surface temperature 1856–1991, *J. Geophys. Res.*, *103*, 18,567–18,589, doi:10.1029/97JC01736.

Kessler, W. S. (2001), EOF representations of the Madden–Julian oscillation and its connection with ENSO, *J. Clim.*, *14*, 3055–3061, doi:10.1175/1520-0442(2001)014<3055:EROTMJ>2.0.CO;2.

Kinter, J. L., III, K. Miyakoda, and S. Yang (2002), Recent change in the connection from the Asian monsoon to ENSO, *J. Clim.*, *15*, 1203–1215, doi:10.1175/1520-0442(2002)015<1203:RCITCF>2.0.CO;2.

Klein, S. A., B. J. Soden, and N.-C. Lau (1999), Remote sea surface temperature variations during ENSO: Evidence for a tropical atmospheric bridge, *J. Clim.*, *12*, 917–932, doi:10.1175/1520-0442(1999)012<0917: RSSTVD>2.0.CO;2.

Kumar, K. K., B. Rajagopalan, and M. A. Cane (1999), On the weakening relationship between the Indian Monsoon and ENSO, *Science*, *284*, 2156–2159, doi:10.1126/science.284.5423.2156.

Li, T., Y. S. Zhang, C. P. Chang, and B. Wang (2001), On the relationship between Indian Ocean SST and Asian summer monsoon, *Geophys. Res. Lett.*, *28*, 2843–2846, doi:10.1029/2000GL011847.

Locarnini, R. A., A. V. Mishonov, J. I. Antonov, T. P. Boyer, H. E. Garcia, O. K. Baranova, M. M. Zweng, and D. R. Johnson (2010), *World Ocean Atlas 2009*, vol.1, *Temperature*, NOAA Atlas NESDIS, vol. 68, edited by S. Levitus, 184 pp., U.S. Gov. Print. Off., Washington, D. C.

Ma, J., and J. Li (2008), The principal modes of variability of the boreal winter Hadley cell, *Geophys. Res. Lett.*, *35*, L01808, doi:10.1029/2007GL031883.

McPhaden, M. J. (2004), Evolution of the 2002/03 El Niño, *Bull. Am. Meteorol. Soc.*, *85*(5), 677–695, doi:10.1175/BAMS-85-5-677.

Meehl, G. A. (1987), The annual cycle and interannual variability in the tropical Indian and Pacific Ocean regions, *Mon. Weather Rev.*, *115*, 27–50, doi:10.1175/1520-0493(1987)115<0027:TACAIV>2.0.CO;2.

Meehl, G. A. (1993), A coupled air-sea biennial mechanism in the tropical Indian and Pacific regions: Role of oceans, *J. Clim.*, *6*, 31–41, doi:10.1175/1520-0442(1993)006<0031:ACASBM>2.0.CO;2.

Meng, X., and D. Wu (2002), Contrast between the climatic states of the warm pool in the Indian Ocean and in the Pacific Ocean, *J. Ocean Univ. China*, *1*, 119–124, doi:10.1007/s11802-002-0003-y.

Parthasarathy, B., A. A. Munot, and D. R. Kothawale (1994), All-India monthly and seasonal rainfall series: 1871–1993, *Theor. Appl. Climatol.*, *49*, 217–224, doi:10.1007/BF00867461.

Picaut, J., M. Ioualalen, C. Menkes, T. Delcroix, and M. J. McPhaden (1996), Mechanism of the zonal displacements of the Pacific warm pool: Implications for ENSO, *Science*, *274*, 1486–1489, doi:10.1126/science.274.5292.1486.

Pierrehumbert, R. T. (1995), Thermostats, radiator fins, and the runaway greenhouse, *J. Atmos. Sci.*, *52*, 1784–1806, doi:10.1175/1520-0469(1995)052<1784:TRFATL>2.0.CO;2.

Ramanathan, V., and W. Collins (1991), Thermodynamic regulation of ocean warming by cirrus clouds deduced from observations of the 1987 El Niño, *Nature*, *351*, 27–32, doi:10.1038/351027a0.

Rayner, N. A., D. E. Parker, E. B. Horton, C. K. Folland, L. V. Alexander, D. P. Rowell, E. C. Kent, and A. Kaplan (2003), Global analyses of sea surface temperature, sea ice, and night marine air temperature since the late nineteenth century, *J. Geophys. Res.*, *108*(D14), 4407, doi:10.1029/2002JD002670.

Saji, N. H., and T. Yamagata (2003), Possible impacts of Indian Ocean dipole mode events on global climate, *Clim. Res.*, *25*, 151–169, doi:10.3354/cr025151.

Saji, N. H., B. N. Goswami, P. N. Vinayachandran, and T. Yamagata (1999), A dipole mode in the tropical Indian Ocean, *Nature*, *401*, 360–363, doi:10.1038/43854.

Sardeshmukh, P. D., and B. J. Hoskins (1988), The generation of global rotational flow by steady idealized tropical divergence, *J. Atmos. Sci.*, *45*, 1228–1251, doi:10.1175/1520-0469(1988)045<1228:TGOGRF>2.0.CO;2.

Schneider, N., T. Barnett, M. Latif, and T. Stockdale (1996), Warm pool physics in a coupled GCM, *J. Clim.*, *9*, 219–239, doi:10.1175/1520-0442(1996)009<0219:WPPIAC>2.0.CO;2.

Smith, T. M., R. W. Reynolds, T. C. Peterson, and J. Lawrimore (2008), Improvements to NOAA's historical merged land-ocean surface temperature analysis (1880–2006), *J. Clim.*, *21*, 2283–2296, doi:10.1175/2007JCLI2100.1.

Sun, D.-Z. (2003), A possible effect of an increase in the warm pool SST on the magnitude of El Niño warming, *J. Clim.*, *16*, 185–205, doi:10.1175/1520-0442(2003)016<0185:APEOAI>2.0.CO;2.

Wallace, J. M. (1992), Effect of deep convection on the regulation of tropical sea surface temperature, *Nature*, *357*, 230–231, doi:10.1038/357230a0.

Wang, H., and M. Metha (2008), Decadal variability of the Indo-Pacific warm pool and its association with atmospheric and oceanic variability in the NCEP-NCAR and SODA reananlyses, *J. Clim.*, *21*, 5545–5565, doi:10.1175/2008JCLI2049.1.

Webster, P. J., and R. Lukas (1992), TOGA COARE: The coupled ocean atmosphere response experiment, *Bull. Am. Meteorol. Soc.*, *73*, 1377–1416, doi:10.1175/1520-0477(1992)073<1377:TCTCOR>2.0.CO;2.

Webster, P. J., A. M. Moore, J. P. Loschnigg, and R. R. Leben (1999), Coupled oceanic-atmospheric dynamics in the Indian Ocean during 1997–98, *Nature*, *401*, 356–360, doi:10.1038/43848.

Webster, P. J., G. J. Holland, J. A. Curry, and H. R. Chang (2005), Changes in tropical cyclone number, duration, and intensity in a warming environment, *Science*, *309*, 1844–1846, doi:10.1126/science.1116448.

Williams, P., and C. Funk (2011), A westward extension of the warm pool leads to a westward extension of the Walker circulation, drying eastern Africa, *Clim. Dyn.*, *37*, 2417–2435, doi:10.1007/s00382-010-0984-y.

Wyrtki, K. (1989), Some thoughts about the West Pacific Warm Pool, in *Proceedings of Western Pacific International Meeting and Workshop on TOGA COARE*, edited by J. Picaut, et al., pp. 99–109, Inst. Fr. de Rec. Sci. pour le Dév. en Coop., Cent. de Nouméa, Nouméa, New Caledonia.

Xie, S.-P., H. Annamalai, F. A. Schott, and J. P. McCreary (2002), Structure and mechanisms of South Indian Ocean climate variability, *J. Clim.*, *15*, 864–878, doi:10.1175/1520-0442(2002)015<0864:SAMOSI>2.0.CO;2.

Xie, S.-P., K. Hu, J. Hafner, H. Tokinaga, Y. Du, G. Huang, and T. Sampe (2009), Indian Ocean capacitor effect on Indo–western Pacific climate during the summer following El Niño, *J. Clim.*, *22*, 730–747, doi:10.1175/2008JCLI2544.1.

Xie, S.-P., Y. Du, G. Huang, X.-T. Zheng, H. Tokinaga, K. Hu, and Q. Liu (2010), Decadal shift in El Niño influences on Indo–western Pacific and East Asian climate in the 1970s, *J. Clim.*, *23*, 3352–3368, doi:10.1175/2010JCLI3429.1.

Yang, J., Q. Liu, S.-P. Xie, Z. Liu, and L. Wu (2007), Impact of the Indian Ocean SST basin mode on the Asian summer monsoon, *Geophys. Res. Lett.*, *34*, L02708, doi:10.1029/2006GL028571.

Yu, J.-Y., and K. M. Lau (2005), Contrasting Indian Ocean SST variability with and without ENSO influence: A coupled atmosphere-ocean GCM study, *Meteorol. Atmos. Phys.*, *90*, 179–191, doi:10.1007/s00703-004-0094-7.

Zhang, C. (1993), Large-scale variability of atmospheric deep convection in relation to sea surface temperature in the Tropics, *J. Clim.*, *6*, 1898–1913, doi:10.1175/1520-0442(1993)006<1898:LSVOAD>2.0.CO;2.

S. T. Kim and J.-Y. Yu, Department of Earth System Science, University of California, 3315 Croul Hall, Irvine, CA 92697, USA. (seontk@uci.edu)

M.-M. Lu, Research and Development Center, Central Weather Bureau, 64 Kong-yuang Rd., Taipei 10048, Taiwan.